

Calculations of Photospheric Plasma Velocity Fields Using Photospheric Magnetic Field Measurements

J. C. Santos, J. Büchner and B. Nikutowski

*Max-Planck-Institut für Sonnensystemforschung, 37191
Katlenburg-Lindau, Germany*

M. V. Alves

*Instituto Nacional de Pesquisas Espaciais, 12227-010 São José dos
Campos-SP, Brazil*

Abstract. The amount of emergence and submergence of magnetized plasma through the photosphere might be crucial for modeling the solar coronal dynamics. It cannot be measured directly since it is too small to produce measurable doppler-shifts. We compare three methods to estimate the photospheric flow from magnetic field observations. The methods are tested using photospheric vector magnetic field data for active region NOAA 8210.

1. Introduction

The Solar B mission with its opportunities for vector magnetic field measurements and rich onboard plasma diagnostics will provide excellent opportunities to investigate the dynamics of the solar corona including eruptions above active regions. Numerical modelling is necessary, however, to connect photospheric magnetic field observations and the coronal dynamics, particle acceleration and heating which will be observed simultaneously by XRT and EIS (Büchner 2004). As a boundary condition for realistic models it will be necessary to know, however, the photospheric plasma flows and the magnetic field evolution. Indeed, photospheric plasma and magnetic field evolution are closely related due to the large values of the magnetic Reynolds number in this region. Hence, the photospheric plasma velocity field can be estimated from the evolution of magnetic features. Several methods have been suggested to calculate the photospheric plasma velocity field from a sequence of photospheric magnetograms, see, e.g. November & Simon (1988), Kusano et al. (2002), Welsch et al. (2004), Longcope (2004), Georgoulis & LaBonte (2004). We compare three methods: Local Correlation Tracking - LCT (November & Simon 1988), ILCT - a combination of induction equation and LCT (Welsch et al. 2004) and MEF - the Minimum Energy Fit method (Longcope 2004). The methods are applied to vector magnetograms from AR8210 obtained on May 1st 1998, between 17:13 UT and 21:29 UT. The velocity field for AR8210 was already obtained by Welsch et al. (2004) and Longcope (2004) but for different regions and time intervals. Here we apply the different methods to the same region and time interval and compare the resulting velocity fields.

2. The Methods

2.1. Local Correlation Tracking (LCT)

This technique was introduced into solar physics by November & Simon (1988). The idea of the LCT method is to find the displacement that maximizes the spatially localized cross-correlation function between two images of a scene separated by a sampling time delay τ , that is smaller than the lifetime of tracers in the scene. The localized cross correlation function is given by

$$C(\vec{\delta}, \vec{r}) = \int J_t(\vec{\epsilon} - \frac{\vec{\delta}}{2}) J_{t+\tau}(\vec{\epsilon} + \frac{\vec{\delta}}{2}) W(\vec{r} - \vec{\epsilon}) d\vec{\epsilon} \quad (1)$$

where $\vec{\delta}$ is the displacement, \vec{r} is the central location of the window, J is the intensity image and $\vec{\epsilon}$ is the location of the pixels relative to the center of the window. The integration is effectively limited in extent to the size of the window function W . The size of the window is chosen to include the basic tracer features.

As discussed by Demoulin & Berger (2003), the LCT method may incorporate some apparent motion that does not correspond to actual horizontal flows, but is caused by the emergence of inclined magnetic structures. This happens because the LCT method considers only the vertical magnetic field component and assumes its changes to be caused by a horizontal plasma motion. Based on geometrical arguments they suggested a correction to the LCT velocity, given by

$$\vec{u}_h = \vec{v}_h - \frac{v_v}{B_v} \vec{B}_h \quad (2)$$

where the subscript h mean horizontal component, the subscript v the vertical component and \vec{B}_h is the projection of the full vector magnetic field to the horizontal plane. The velocities v_v and v_h are the vertical and the horizontal component of the "real" velocity, respectively, while u_h is the horizontal component of the apparent velocity, in this case the LCT velocity.

2.2. A combination of LCT with induction equation(ILCT)

In order to take into account also upward and downward moving plasmas, Kusano et al. (2002) and Welsch et al. (2004) considered the magnetic field evolution and plasma motion consistent with the vertical component of the induction equation. Combining the induction equation and the Démoulin & Berger relation they obtained:

$$\frac{\partial B_v}{\partial t} = \vec{\nabla}_h \cdot (v_v \vec{B}_h - B_v \vec{v}_h) = -\vec{\nabla}_h \cdot (\vec{u}_h B_v). \quad (3)$$

Decomposing the flow vector field $\vec{u}_h B_v$ in terms of two scalar potentials

$$\vec{u}_h B_v \equiv \vec{\nabla}_h \times \psi \hat{n} - \vec{\nabla}_h \phi, \quad (4)$$

one obtain two Poisson equations for the scalar potentials ϕ and ψ

$$\nabla_h^2 \phi = \frac{\partial B_v}{\partial t} \quad (5)$$

$$\nabla_h^2 \psi = -\vec{\nabla}_h \times [\vec{u}_h B_v] \cdot \hat{n} \quad (6)$$

Using $\vec{u}^{(LCT)}$ as a first approximation for \vec{u}_h and solving the equations (5) and (6) for ϕ and ψ , equation (4) can be used to obtain an improved estimate of \vec{u}_h .

2.3. Minimum Energy Fit (MEF)

This technique, introduced by Longcope (2004) also uses the vertical component of the induction equation and selects the solution that minimizes the functional

$$W\{\psi, v_v\} \equiv \frac{1}{2} \int_M [|\vec{v}_h - \vec{u}_h|^2 + |v_z - u_z|^2] dx dy, \quad (7)$$

where $\vec{u}(\vec{r}_h)$ is a lower order reference flow and ψ is the scalar potential defined in equation (4).

3. Results

We calculated the flow velocities for the same area encircling AR8210 by all three methods. Figure 2 shows a vector magnetogram of AR8210 obtained on May 1st 1998, 17:13 UT (upper, left panel), and the variation of the normal magnetic field component between 17:13 UT and 21:29 UT (upper, right panel). It also shows the velocity field resulting from the application of the ILCT method (middle, left panel), MEF method (lower, left panel) and the variation of the normal component of the magnetic field, computed using these velocity field and the induction equation. The results for the horizontal component if the velocity obtained by LCT method are presented in Figure 1.

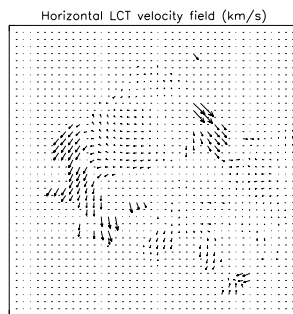


Figure 1. Horizontal velocity field pattern obtained using LCT method for the evolution of AR8210.

Plasma flow velocities were calculated only if the normal component of the magnetic field was larger than 100G. The LCT results for the horizontal velocity present a mean velocity of 0.01 km/s, with a maximum value of 0.32 km/s. The horizontal mean and maximum velocity using ILCT were 0.03 km/s and 0.5 km/s. MEF revealed much larger horizontal velocities, values larger than 5 km/s were disregarded. For the vertical velocity the maximum values obtained were 0.3 km/s and 4.5 km/s with mean values of 0.005 km/s and 0.009 km/s, respectively for ILCT and MEF.

4. Conclusions

While the resulting velocity values calculated using ILCT and MEF methods differ from each other, both the overall structure of the velocity fields and the variation of the resulting normal component of the magnetic field that they produce is very similar. This means that we can use both results as representing the velocity field responsible by the evolution of the normal component of the magnetic field but have to worry about the absolute value of the velocities. As both methods require that the resulting velocity fields satisfy the induction equation they are appropriate to be used for providing an input information to solar MHD simulations, and probably a combination of them would be the best option for future realistic models helping to understand the Solar B observations.

References

- Büchner, J., 2006, Modelling solar reconnection by connecting photospheric observations and microscopic theory, This Solar-B volume.
Démoulin, P., Berger, A. 2003, Solar Physics, 215, 203
Georgoulis, M.K., LaBonte, B.J. 2004, preprint
Kusano, K., Maeshiro, T., Yokoyama, T., Sakurai, T. 2002, Astrophys. J., 577, 501
Longcope, D.W. 2004, Astrophys. J., 612, 1181
November, L.J., Simon, G.W. 1988, Astrophys. J., 333, 427
Welsch, B.T., Fisher, G.H., Abbet, W.P., Regnier, S. 2004, Astrophys. J., 610, 1148OA

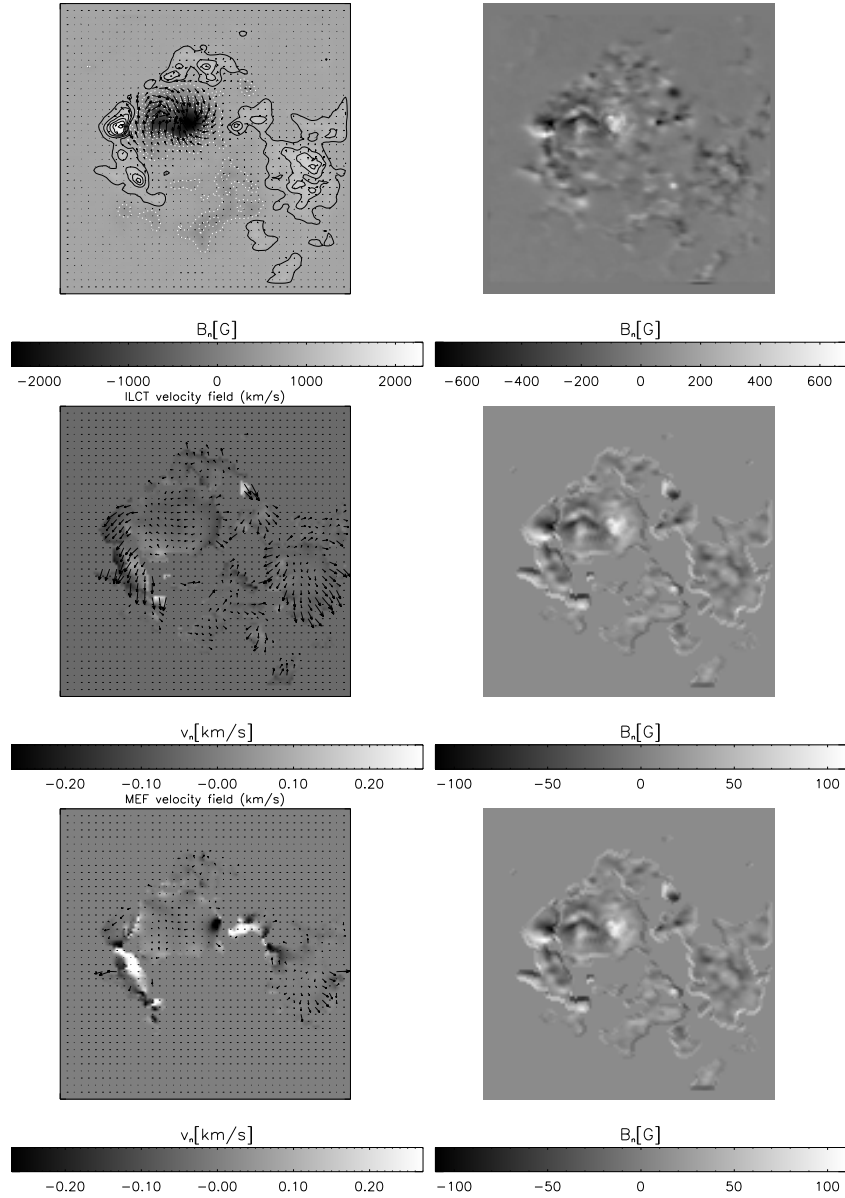


Figure 2. Top left - vector magnetograph of AR8210 obtained in may 1st 1998 - 17:13 UT; Top right - variation of the normal component of the magnetic field between the interval 17:13 UT - 21:29 UT; Center left - velocity field obtained using ILCT method; Center right - variation of the magnetic field normal component obtained using ILCT velocity field; Botton left - velocity field obtained using MEF method; Botton right - variation of the magnetic field normal component obtained using MEF velocity field.